ABSTRACT

Halley-type comets tend to have a series of dust trails that remain spatially correlated for extended periods of time, each dating from a specific return of the comet. Encounters with 1 - 9 revolution old individual dust trails of 55P/Tempel-Tuttle have led to well recognized Leonid shower maxim, the peak time of which was well predicted by recent models. Now, we used the same model to calculate the position of dust trails of comet 8P/Tuttle, a Halley-type comet in a ~13.6-year orbit passing just outside of Earth's orbit. We discovered that the meteoroids tend to be trapped in the 14:12 mean motion resonance with Jupiter, while the comet librates in a slightly shorter period orbit around the 13:15 resonance. It takes 6 centuries to change the orbit enough to intersect Earth's orbit. During that time, the meteoroids and comet separate in mean anomaly by 6 years, thus explaining the unusual aphelion occurrences of Ursid outbursts. The resonances also prevent dispersion, so that the dust trail encounters (specifically from dust trails of AD *1378 - 1405*) occur only in one year in each orbit. We predicted enhanced activity on December 22, 2000, at around 7:29 and 8:35 UT from dust trails dating to the *1405* and *1392* return, respectively. This event was observed from California using video and photographic techniques. At the same time, five Global-MS-Net stations in Finland, Japan and Belgium counted meteors using forward meteor scatter. The outburst peaked at 8:06±07 UT, December 22nd, at Zenith Hourly Rate ~ 90 per hour. The Ursid rates were above half peak intensity during 4.2 hours. This is only the second Halley type comet for which a meteor outburst can be dated to a specific return of the parent comet, and traces their presence back form 9 to at least 45 revolutions of the comet. New orbital elements of Ursid meteoroids are presented. We find that most orbits do scatter around the anticipated positions, confirming the link with comet 8P/Tuttle and the epoch of ejection. The *1405* and *1392* dust trails appear to have contributed similar amounts to the activity profile. Some orbits provide a hint of much older debris being present as well. Some of the dispersion in the radiant position may reflect a true variation in inclinations, with two groupings at low and high values, which is not understood at present.

1. INTRODUCTION

Advances in understanding the dynamics of comet dust trails and their manifestation as meteor showers on Earth have recently evolved to the point where some types of meteor outbursts can now be assigned to ejecta of specific epochs of the parent comet. Point in case are the Leonid meteor storm of November 18, 1999, and a second outburst half a day later, which were assigned to ejecta of comet 55P/Tuttle during the returns of 1899 and 1866, respectively (Kondrat'eva and Reznikov 1985, Lyytinen 1999, McNaught and Asher 1999). The Leonid return in 2000 showed three outbursts, identified with ejections from 1932, 1733 and 1866 (Lyytinen and Van Flandern 2000). All outbursts are the result of Earth crossing a narrow trail of dust put in Earth's path as a result of planetary perturbations (Kresák 1993,Williams and Wu 1994, Jenniskens 1995, 1997, 1998a, Jenniskens et al. 1997).

The work to date only serves as a framework for comprehensive models that can correctly predict the time, peak activity, duration, and particle size distribution of the meteor outbursts. One of the questions that need to be addressed is the role of mean motion resonances in the orbital evolution of the trails. While (fragments of) young dust trails may escape close encounters with Jupiter, older trails tend to maintain their cohesion only if the meteoroids continue to avoid dynamically unfavorable conditions. Asher et al. (1999) pointed out that dust trails could maintain their character for a very long time when the particles are trapped in mean-motion resonances.

During a cold winter night in December of 1986, Norwegian observer Kai Gaarder and Lars Trygve-Heen saw a spectacular outpour of Ursid meteors over a period of 3 hours (Jenniskens 1987). Visual observers at Skalnaté Pleso Observatory in 1945 (Becvár 1946) had reported a similar outburst. Ceplecha (1951) calculated the orbital elements of the meteors from three single-station trajectories and an assumed velocity and found good general agreement with the orbit of comet 8P/Tuttle. This confirmed an earlier notion by W.F. Denning, who had observed a

minor annual meteor shower in Ursa Minor (Denning 1912), but the weak nature of the shower prompted him to add that such a relationship "may be an accidental accordance" (Denning 1921).

8P/Tuttle is a Halley-type comet with an orbital period of about 13.6 years, which during its most recent return in 1994 has passed outside of Earth's orbit at a relatively large distance of +0.061 AU (Marsden 1995). These Ursid outbursts are very unusual, because they occur when the parent comet 8P/Tuttle is near aphelion. This is such a strange phenomenon that we assigned "far-comet" status to these outbursts in our earlier study (Jenniskens 1995). We now know that other far-comet type outbursts are associated with long-period comets, instead, leaving the Ursid case an orphan.

The comet was about to be back at aphelion in March of 2001, when we considered the possibility of another Ursid outburst in December 2000. Application of the Leonid shower prediction models to the Ursids in early December revealed that Earth was about to cross the dust trails of *1405* and *1392* on December 22, 2000. If confirmed, this would be only the third time that meteors are traced to a specific epoch of ejection (following Leonid and Draconid predictions). Moreover, the predictions identified dust trails about 328 years older than any trails discussed to date. Still, on the time scale of space weathering, these Ursid meteoroids, just like the Leonids, are relatively fresh cometary ejecta, not much affected by weathering in the interplanetary medium.

The prediction was summarized in a December 2000 issue of *WGN, the Journal of the IMO*, a preprint of which was widely circulated on the internet and in the astronomical community prior to the shower (Jenniskens and Lyytinen 2000). An announcement was made as well in the IAU Circular (Jenniskens 2000a). In order to confirm the forecast, video and photographic observations were deployed in California, while radio forward meteor-scatter observers worldwide gathered meteor counts. Early reports on those observations confirm that an outburst occurred around the predicted time at the anticipated level of activity (Jenniskens 2000b, Jenniskens and Lyytinen 2001).

This paper elaborates on these early papers by comparing the results of the observations to the predictions that were made. New results from the video observations are presented. We will discuss the role of mean motion resonances in the orbital evolution of the Ursid dust trails 44 and 45 revolutions after ejection from the comet and conclude that the observations may show a more complex scenario than originally envisioned.

2. PRIOR OBSERVATIONS

The Ursid Filament

Let us first examine other manifestations of the Ursid shower in recent years, to show the unusual aspects of these aphelion outbursts. The annual Ursid shower has a peak Zenith Hourly Rate (ZHR) of = 8 hr^{-1}, and has a ZHR > 1 hr^{-1} between about December 18 to 25 (Jenniskens 1994). Planetary perturbations have dispersed this dust sufficiently wide and all along the comet orbit for annual encounters with Earth. This component represents a minimum activity in such quiet years as 1998 and 1999.

On top of that, there are frequent outbursts when the comet is near perihelion. Figure 1 shows the rate of meteors detected by forward meteor-scatter above the normal daily activity between December 19 to 24. Shortly before the comet's return in December 1993, Bob Lunsford of Mt. Laguna, California, observed the ascending branch of an outburst rising to ZHR_{max} = 100 hr^{-1}. The meteors were of average brightness, with a magnitude distribution index r = N(m+1)/N(m) = 2.5. Japanese observer H. Shioi observed the peak the next year in 1994 (Ohtsuka et al. 1995), from which we have ZHR_{max} = 50 hr^{-1} (r = 2.6). After that, rates gradually declined. In 1996, rates were still elevated at ZHR_{max} = 25 hr^{-1} (Langbroek 1997), and of order ZHR_{max} = 16 hr^{-1} in 1997 (our work). No significant enhanced activity over the normal annual shower rates occurred in 1999. Moreover, similar outbursts were observed during the previous return of the comet, by Japanese observers in 1981 (Ohtsuka 1994) and by Jos Nijland and Hans Breukers of the Dutch

Meteor Society in 1982, who observed the descending branch starting at ZHR ~ 35 hr^{-1} (our work).

These perihelion outbursts occurred at a significantly different point in the orbit than the 1986 outburst, about 6 hours earlier, and were significantly wider. We have B = 2.5±0.5 $degree^{-1}$ if the zenith hourly rate has the functional form (Jenniskens 1994):

$$ZHR \sim 10^{-B|\lambda_o-\lambda_{omax}|} \quad (1)$$

with solar longitude λ_o a measure of time, or a Lorenz curve width of full-width-at-half-maximum W = 0.35±0.05° if the function form is a Lorentz profile as in the case of the 1999 Leonid meteor storm (Jenniskens et al. 2000):

$$ZHR \sim (W/2)^2 / ((\lambda_o-\lambda_o^{max})^2-(W/2)^2) \quad (2)$$

The Lorentzian curve adds a tail to the exponential center that is well described by Eq. 1. The width is wider than for typical dust trail encounters of the Leonids and Draconids, which have a full-width-at-half-maximum about a factor of ten smaller (Jenniskens 1995).

The activity profiles describe the nodal distribution of the orbits and dispersion of dust along the comet orbit. The only other information on the dynamical properties of this dust are a series of thirteen outburst Ursid orbits obtained from two-station video observations in California over a period of 4 hours in December of 1997 (Table I - orbits with prefix "97"). The radiants of these orbits show significant scatter with a wide range in Right Ascension, more than in Declination, even without 3 possible outlayers (Fig. 2). The mean of the ten orbits that are most clustered is listed in Table II. This suggests significant planetary perturbations, consistent with the relatively large nodal dispersion. Also, note that the orbits significantly differ from that calculated by Ceplecha for the 1945 Ursid outburst (Table II).

Aphelion Outbursts

The aphelion outbursts (Figure 3) happened when the comet was near aphelion and, remarkably, stood alone with no other outbursts in 1946 (Ceplecha 1951) and no sign of an outburst in radio-MS data in 1987 (Jenniskens 1988c). The 1945 outburst happened 6.089 yr. after perihelion

passage in 1939, Nov. 10.6 (1939 X), while the 1986 outburst happened 6.002 years after the 1980, Dec. 14.7 perihelion passage of comet 1980 XIII. Compare this to the anticipated encounter in 2000, which occurred 6.549 yr. after the 1994, June 25.3 passage of the parent comet.

These aphelion outbursts are much more narrow than the perihelion outbursts discussed in the previous section, by a factor of 6, with $B = 17\pm3$ degree^{-1} rather than $B = 2.5$ degree^{-1}, or a Lorentz width of $W = 0.05\pm0.01°$. Note the difference in scale in Figures 1b and 3. Also, the magnitude distribution index may have been slightly steeper. From Kai Gaarder's magnitude estimates, we have $r = 2.8$ (Jenniskens 1988c).

3. ANTICIPATED ACTIVITY IN DECEMBER 2000

We submit that the broad 1981-82 and 1993-1997 perihelion outbursts are probably the accumulation of dust from multiple debris trails, with dust in orbital resonances, forming a structure much like the Leonid and Perseid Filaments of other Halley-type comets (Jenniskens and Betlem 2000). This accumulation has occurred over a relatively long period of time. For example, Brown and Arlt (2000) derived an accumulation age stretching from AD 400 until 1700 for the Leonid Filament. In the process, the signature of individual trails is lost.

Given the much more narrow width of the aphelion outbursts, on the other hand, it is not unreasonable to argue that the material responsible for the 1986 outburst is not very old, and can probably be traced back to a single dust trailet. Similarly, the 1945 outburst might well be identified with a single dust trailet.

That hypothesis has the exciting prospect of predicting possible Ursid outbursts in December of 2000 and beyond, analog to recent predictions of Leonid returns (Lyytinen & Van Flandern 2000). In recent years, relatively simple meteoroid stream models have been developed that have proven very successful in predicting the encounter of Earth with comet dust trails of 1- 4 revolutions old, but with less good results for dust trails 5 - 9 revolutions old (Kondrat'eva & Reznikov 1985, McNaught & Asher 1999, Lyytinen 1999). Recently, we worked to improve the models in order to have a better agreement with observations for these somewhat older trails by including non-gravitational effects due to radiation pressure (such as the seasonal Yarkovski effect) that continue to accelerate the grains over time, called the "A2 effect" in analogy with the effects of mass loss on comet orbit dynamics (Lyytinen and Van Flandern 2000). In our model, the A2 effect is simulated by slightly changing the speed of the meteoroids at each perihelion, the magnitude of which is determined by our Leonid observations in 2000 (Lyytinen et al., in prep.).

We were now ready to take that model a step further and consider dust trails of several tens of orbits old. Comet 8P/Tuttle has an orbit outside of Earth's orbit. For a meteoroid to hit Earth, the particle's perihelion distance (q) has to move inward to the Sun. Our investigation of the orbital dynamics of the Ursid meteoroids show that only trails no younger than several hundred years back intersect Earth's orbit today.

As before, we calculated the orbital evolution of dust trails ejected over the past 800 years ending up in orbital resonances close to that of the comet. The J2000 planetary orbits were adopted from the JPL database. The comet orbit was taken from the IAU Minor Planet Center database (Marsden 1995). The comet and planet orbits were backward integrated for 2000 yrs, allowing for the non-gravitational A2 term and for the gravitational effects of the planets. We used an orbit integrator of our own design. The A1 parameter was not modeled because it has very little effect on the orbit integrations. Then we generated orbits of test particles having the orbital elements of the comet at perihelion, but having different semi-major axis ($a+\Delta a$), and

integrated those orbits to the present time (using the gravitational effects of the major planets except Pluto).

We plotted the resulting differences between the radial distance of dust trail and Earth (rD-rE) as a function of perihelion time; this type of plot giving a rapid overview over even the most chaotic trails. For example, figure 4 shows the position of the dust particles of the *1392* dust ejecta in time of ecliptic plane crossing (horizontal axis) and space in terms of rD-rE around the time of the December 1945 outburst. In contrast to the recent trails for the Leonids or Draconids, these ancient dust trails are far from well-behaved lines. Close encounters with Earth cause frequent gaps in the trails. Sometimes, there are more or less conserved trail fragments (trailets), but in other cases a chaotic cloud of particles is all that remains as a result of planetary perturbations on an old trail. Neighboring particles in this cloud may have quite different orbital elements, which makes the prediction of peak times uncertain.

The results were checked by Hartwig Leuten (Priv. Comm.) using a model including both the A1 and A2 terms and using the K11 orbit integrator, version 3.0 by Christian Clowinski at an accuracy factor of 50 (for the comet integration) or 25 (or the trail computation), and found in good agreement with our calculations, with less than 0.0001 AU difference in rD-rE after 46 revolutions.

Inspecting the historic variations of q of the parent comet, we find maybe a dozen returns that could have resulted in a dust trail close to Earth's orbit at the present time. We examined a number of those trails to identify the ones likely to cause an outburst (Figure 4). Of course, many trails from encounters further back in time may contribute as well, but those should be less significant.

The dust from 1392 can account for the 1945 outburst, when the miss distance was less than rD-rE = +0.001 AU (Figure 5). The trail is still well behaved at the point of intersection, indicated by an arrow. The computed maximum from the model, Dec. 22, 18:29 UT, is compatible with the meteor stream activity curve plotted in Jenniskens (1995), although the descending arm of

this curve remained unobserved. Integration forward to 2000 shows that this same trail can perhaps produce a meteor outburst in December 2000 at solar longitude 270.808 (J2000). However, the miss distance (rD-rE) has increased to +0.0038 AU (Fig. 4). Note that in our earlier calculations, which did not include the A2 effect, we found a slightly smaller miss distance of +0.0035 AU (Jenniskens and Lyytinen 2000).

We find that a trail from dust ejected 44 revolutions back in the year 1378 is the likely source of the 1986 outburst (Figure 6). The trail comes close to Earth's orbit and the timing is to within 0.01° from the observed value. This particular trail folds on itself and a 100 times higher local density of model particles is needed to get a good view of the position of the trail near Earth's orbit. Figure 6 shows two small trail fragments that approach Earth's orbit at the time of the December 1986 Ursid outburst. The first trailet (top Fig. 6) shows a regular course, with the exception of two test particles. The orbital elements of the particles near the intersection (cross) have a node at 270.934 (J2000), which is close to the peak of Figure 3. The trailet is stretched out significantly at the point of intersection, which would have lowered the expected dust density. We conclude that if the encounter had been a few weeks later, the Ursid shower would have been 1-2 orders of magnitude more intense. The second fragment of the *1378* trail (Figure 5b), with a higher original Δa, does also encounter Earth at the expected time. This trailet was sampled with a particle density of only 40 times higher than normally used. The encounter is at 270.816 (2000.0). The trail is less stretched out and would have given higher dust densities, but the dust density falls off exponentially with Δa, adding up to a factor of 10 compared to the first trailet dust density. This would account for the lower observed ZHR ~ 20 at that time. The observations are not sufficiently accurate to tell if this trailet was there. The same trail is near Earth's orbit as well in December of 2000, when the encounter occurs at solar longitude 270.82 (J2000), but at a distance of +0.0069 AU and at +0.025 AU for the two trailets, respectively (Figure 4).

Rather, it is the next 45 revolution old trail (to this year) of 1405 that is a prime candidate for an outburst in December 2000. Figure 7 shows in a dense model that a well-behaved trail segment is near Earth's orbit at the time of the December 2000 encounter. It has a small rD-rE = -0.0013 AU at solar longitude 270.759 (J2000). The trail curves on itself right at that point in time and the

local dust density is relatively high. In our initial study (Jenniskens and Lyytinen, 2000),we did not include non-gravitational perturbations and noticed that the reversion in the dust trail did not reach the point in time of the encounter. If true, the dust would only have start crossing the Earth's orbit a day too late. However, after including the A2 effect, we now confirm that the dense tip of the *1405* dust trail has moved to cover the outburst date without affecting rD-rE (Figure 7).

The Cause of the 6-year Lag

Figure 7 shows a compilation of the dust trails of 1365, 1378, 1392 and 1405, each point representing the crossing of a particle through the ecliptic plane at the given time (X-axis) and at the given distance rD-rE. The y-axis rD-rE = 0 corresponds to Earth's position on December 22 in the given year. We find that the majority of particles is only near Earth's orbit in December of 2000, with no particles nearby in the year before or after. This is in agreement with observations, which showed outbursts only in 1945 and 1986, but not in 1946 and 1987.

The model also has particles encounter Earth only 6 years after the passage of the comet (marked in figure 7). The reason for this is that the particles are mostly trapped in orbital resonances. The comet currently librates around the "high" 13:15 mean motion resonance with Jupiter. Because of radiation pressure effects on the particles, they tend to get into slightly longer orbital periods than the comet and end up trapped in the mean motion resonance 12:14 (= 6:7). Because it takes the particles longer to travel around the Sun, they will gradually move away from the comet. If at these resonances the librations are small, meaning that the particles will keep near the center of the "window", then there will be a systematic decrease of the perihelion distance (q) more rapidly than for the comet itself, ultimately leading to necessary Earth crossing to see an Ursid outburst. This decrease of q is thought to be the result of planetary perturbations from Saturn, and in lesser extend from Uranus and Neptune. Note, however, that near the leading edge of the resonance, the particles may have close encounters with Jupiter that will increase q instead.

We find that it takes about 6 centuries for dust to move close to Earth's orbit. During that time, the separation of the particles and comet in mean anomaly, as a result of the difference in orbital period, increases to 6 years. This is a natural explanation of why the 1986 and 1945 outbursts occurred about 6 years after the comet's closest encounter with Earth's orbit, or near aphelion. We also find that the resonances effectively confine the dust to a single year return, thus explaining the lone nature of the outbursts.

Younger trails than *1405* are found nowhere near Earth's orbit (Fig. 4). The *1419* trail has rD-rE = +0.075, while the next trail from 1433 has rD-rE = +0.084 AU. These particles seem to be pushed mostly into the next resonant window 11:13. Most particles in this resonant window are from early orbits around the years AD 1100 - 1200. We find that these dust trails may cause another Ursid outburst in 2002. Overall, we see particles accumulate mostly in the 6:7 orbital resonance, which may be the main reservoir for particles in the Ursid Filament.

The big difference between the trails from 1405 and 1419 is caused by a Jupiter encounter at about 0.86 AU of the parent comet in 1462. Between the 1460 and 1474 encounters, the perihelion distance of the comet increased +0.026 AU. The particles released in 1419 (that cross the ecliptic at the descending node near Dec 22, 2000) are about two months behind the comet in 1462 and in part share this increase, more so than particles released in 1405. As the difference in rD-rE between both trails is now bigger than about 0.02 AU, it may suggest that the Jupiter encounter sets the particles from 1419 into an unfavorable librational status. The dust particles, that escaped before this into a longer period orbit made a more distant encounter and so got more "advantage" to decrease the perihelion distance. The earlier the particles were ejected, the bigger the advantage. Particles ejected several revolutions earlier got into other unfavorable circumstances. Hence, there was this region of a few revolutions that seemed to be the most favorable to get the particles into the librational window in question and a good start for as small a perihelion distance as possible.

Specific Predictions for the 2000 Encounter

Based on these calculations, we made the following specific predictions for the December 2000 encounter (Jenniskens and Lyytinen, 2000):

1) The most likely trail passage would be with the trail of 1405, expected to peak at 7:29 UT. From recent Leonid observations, we measured a factor of 4 wider trail in the plane of the comet orbit, as schematically shown in Fig. 4 (Jenniskens & Gustafson 2001). That put the Earth smack in the trail. Because the particles of the *1405* trail have relatively high Δa, they were expected to be smaller than during past outbursts in 1945 and 1986, perhaps rather near the visual detection limit under good observing conditions.

2) If the dust trail width in the plane of the comet orbit is just a bit wider, the trailet of 1392 might show up at 8:38 UT. If so, these events probably would make a continuous profile 4-5 hours wide, but could perhaps be recognized separately. Both events favored northern hemisphere observers in the America's. The Moon was out of the way providing for generally good observing conditions.

3) The expected intensity of the shower was hard to predict, not in the least because of the necessary influence of an A2 effect to have any activity at all at the time of the encounter. Both the historic 1945 and 1986 encounters had miss distances rD-rE < 0.001 AU, but the dust densities in the trail according to the mean anomaly factor (as reflected in the spreading of the particles in Figures 5 - 7) seemed to be smaller than in this year. The density in the *1405* trail, however, was relatively large. Because of that, we expected peak rates similar to past outbursts, of order 1 per minute.

4) The *1378*-dust (at 8:59 UT) could also not be ignored, albeit that the expected minimum distances are relatively large (Fig. 4). There is some uncertainty in the *1378* trailet position because the A2 effect has not been studied. This trail shows a relatively rapid increase of rD-rE towards the end of 2000 (figure not shown). Since there are particles around rD-rE = 0 only

about a month or two earlier, it may even be that the A2 effect will help bring those near the Earth at the correct radii, if not otherwise.

4. OBSERVATIONS OF THE 2000 ENCOUNTER

In order to confirm the predictions, observing teams were assembled in California to deploy intensified-video cameras and photographic cameras at two separate sites for multi-station imaging. Low-resolution spectrographs were deployed as well, in the hope of comparing the physical properties of the Ursid meteoroids with those of the Leonids.

In search of clear weather, the two sites were set up 1-hour drive further south than our usual observing sites south of the Bay Area. At Lake San Antonio just south of King City, Mike Koop operated four intensified video cameras (two aimed at 70° elevation and two at 30°, due East), Mike Wilson ran a CCD spectrometer, and Chris Angelos and Peter Gural operated a 13-camera 35mm photographic setup and an all-sky intensified video camera for meteor timing. 74 km to the East, at a site south of Coalinga at the intersection of routes 33 and 41, Peter Jenniskens operated six intensified cameras (4 at 70 °, 2 at 25 ° East) and the low resolution slit-less spectrograph "BETSY", while Ming Li and Duncan McNeill ran a second 13-camera battery. The radiant altitude was around 30°.

In addition, video observations were performed from the Netherlands, in a project by Casper ter Kuile, Klaas Jobse, Robert Haas and Romke Schievink. The first three observers set up the cameras from their home locations in De Bilt (52 07'N, 5 11'E), Oostkapelle (51 34'N, 3 32'E) and Alphen a/d Rijn (52 09'N, 4 40'E), while Romke traveled to the Public Observatory Twente in Lattrop (52 25'N, 6 58'E). The radiant altitude was around 60°. All cameras applied second generation image intensifiers and Hi8 or digital camcorders. During the observations the cameras were pointed at the same spot in the atmosphere to allow for multi-station detections. The images from the camera in Alphen a/d Rijn were not reduced because of apparent misalignments of the camera optics.

Ursid Activity

In the Netherlands visual observers noticed a gradual increase in Ursid rates, marking the onset of the outburst (Figure 9, o). 15 Ursid orbits were calculated (Betlem et al. 1999) and are listed in Table II, with a code name starting with "205". When twilight started interfering, California observers took over. Rates gradually increased, until a peak at about 8 UT. A total of 431 Ursids were detected in a single visual scan of the video tapes amidst 394 other meteors in a total of 28.4 hours of effective observing time. From this data set, the best 42 video Ursid orbits were calculated between 6:45 and 9:08 UT, the brightest only magnitude +1. Results are listed in Table II under code names staring with "207". Despite a significant effort, only two Ursids were photographed and both were not multi-station and only just bright enough to be detected. Four Ursid spectra were recorded with the slit-less spectrograph, all faint. No Ursid was bright enough and well enough placed to give a good signal on the CCD spectrometer.

Figure 9 shows the average number of Ursids counted in ten-minute intervals from eight independent cameras, six at the Coalinga site and two at the King City cite (•). These counts are scaled to the Zenith Hourly Rates calculated from visual observations in the Netherlands (o, left), and similar observations in Japan, calculated by Masaaki Takanash of the Nippon Meteor Society (NMS electronic circular Dec. 2000). Radio meteor scatter observations were provided by five stations of the Global Meteor Scatter Network (Jenniskens 1998b). 10-minute counts were obtained by Esko Lyytinen and Ilkka Yrjölä in Finland, Hiroshi Ogawa and Kazuhiro Suzuki in Japan, and Pierre de Groote in Belgium. The mean of those counts is shown as a dashed line in Figure 9 and corresponds well with the video and visual record.

A Lorentzian curve fitted to the data gives a full width at half maximum of W = 0.09±0.01 degrees (or a duration of 4 - 5 hours) and a peak time at solar longitude = 270.780±0.005 (J2000), or 8h 06±07m UT. The peak activity appears to have been rather high, with ZHR ~ 90, but the high magnitude distribution index and the low radiant altitude (26°) made this a much less impressive shower than the Perseids. From the ratio of sporadics and Ursids, we find r = 3.5±0.5 before 8h UT and r = 2.8±0.3 after 8h UT, assuming all other meteors (sporadics) have r,

= 3.4 (Figure 10). For the high cameras only, we have r ~ 3.2 and r ~ 2.9 respectively. From the Ursid count as a function of magnitude, we have r ~ 2.6 and r ~ 2.4, with r_s ~ 3.0, but this result is sensitive to the assumed magnitude range over which all meteors are detected.

Physical Properties of Ursid Meteors

The outburst Ursids show various signs of a more than usual fragile morphology. This is a familiar property of recent Giacobinid ejecta (Draconids) and Tempel-Tuttle ejecta (Leonids). Apparently, this morphology is not much affected even after 44 revolutions or a total age of about 600 yr. in the interplanetary medium for an orbit with q~0.94. Specifically, we find that the Ursid meteoroids do not penetrate as deep as observed for sporadic meteors and other showers at similar entry velocity. Beginning and End heights are summarized in Figure 11. The best Ursid spectrum at 08:24:54 UT (Figure 12) shows an early release of sodium relative to magnesium in a similar manner as observed before for the storming Leonids and Draconids (Borovicka et al. 1999). It is thought that the sodium-containing minerals are exposed more effectively to the impinging air molecules, or the sputtering plasma, than in normal meteors. One explanation is, that the meteoroids fall apart in small fragments early on in their trajectory.

Another interesting result is the relative strength of the first positive bands of nitrogen, which is a very sensitive thermometer for air plasma equilibrium temperatures (Jenniskens et al. 2000a):

$$I(\text{OI } 777.4 \text{ nm})/I(N_2 \text{ } 700 - 776 \text{ nm}) = 8.85 \times 10\text{-}14 \exp(0.00676 * T)$$

The presence of the N_2 bands (the diffuse emission between the Mg, Na and O lines) implies that the chemical equilibrium temperature for the $N+N \leftrightarrow N_2$ reaction in the meteor wake is not much different from than observed in Leonid meteors that are double the speed of Ursids. While Leonid meteors of about magnitude -1 give T = 4,300±100 K, the spectrum of a +2 Ursid results in T = 4260±100 K.

Ursid Trajectories and Orbits

Radiant positions (defining the orientation of the velocity vector) are most precisely measured. The distribution of radiants is significantly dispersed in Right Ascension and (less so) in Declination (Figure 13). There is no central cluster that is readily identified with the *1405* or *1392* dust trails. There are some possible groupings or filaments, with a cluster of radiants at relatively low RA < 215 degrees and another grouping with DEC < 75.0 degrees. The median radiant position and orbital elements are listed in Table II.

The speed of the meteors scatters around 32.7 km/s (Figure 14), but radiants with low Right Ascension have systematically higher velocity (34.2 km/s). Also, radiants from 1997 that have unusually high Right Ascension tend to have lower velocities (31.9 km/s). The speed of the meteors may contain a systematic error because there is an unknown difference between the mean velocity <V> and the entry velocity before atmospheric deceleration V_{inf}. We have adopted a constant difference of V_{inf} - <V> = +0.34 km/s, consistent with other meteors of similar entry velocity.

While the perihelion distance (q) and argument of perihelion (ω) are mainly determined by the measured radiant position, the inclination (I), eccentricity (e) and semi-major axis (a) are mostly determined by the measured speed. Figure 15 plots the inclination versus perihelion distance for the most precise orbits (σ i < 0.55 degrees). Only representative error bars are shown. The orbital elements of test particles representing the two dust trails of *1405* and *1392* are indicated with open symbols. The observed orbits scatter around the calculated positions of both trails, and not only around the *1405* trail. There is a separate cluster of orbits with significantly lower perihelion distance. Those correspond to the low RA < 215 degree (Fig. 13) and high velocity (Fig. 14) outlayers. Although these orbits were mostly observed after 8h UT, they do not refer to the *1392* dust trail, which has slightly larger perihelion distance than the *1405* dust trail. Rather, given the lower perihelion distance, we assume that they are due to even older trails.

The distribution with semi-major axis is shown in Figure 16. There is a strong concentration of orbits near 1/a = 0.21. That peak is at a smaller semi-major axis than the expected value of 1/a = 0.1734 (6:7) or 1/a = 0.1747 for the comet orbit. There may be further concentrations at 1/a = 0.28 and 1/a = 0.15. If we allow for a systematic error in the velocity measurements, a correction to the geocentric speed of +0.29 km/s, ~+0.8 km/s and ~-0.2 km/s is needed, respectively. Such differences are quite reasonable and may reflect variations in the particle surface-to-mass ratio or fragmentation properties. If so, then we find that the older dust trail meteoroids do not appear to contain grains with the highest surface-to-mass ratio.

5. DISCUSSION

Until now, the association of the Ursids with comet 8P/Tuttle depended on the comparison between Ursid orbits and comet orbit, leading to disagreement between comet perihelion distance and comet node (Table II). That situation does not change with the new measurements, because the meteoroid orbits have to be different from the comet orbit in order to intersect Earth's orbit. However, now we can compare the Ursid orbits to the median orbit of the test particles in the *1405* dust trail model. We find good agreement in all orbital elements, within the error bars. The link between the Ursid shower and 8P/Tuttle has been established beyond doubt.

The return of the Ursids demonstrates that the basic approach of current models is valid even for trails dating back as many as 45 orbital revolutions. We can not differentiate between the *1405* and *1392* dust trails. The observations of node and orbital elements suggest that both trails contributed to the December 2000 outburst. The *1378* trail was not detected. The observed activity profile peaks exactly in between the predicted times for the *1405* and *1392* dust trails, as expected if both trails contribute to the profile, and the radiant position scatters around the expected positions of both trails. Indeed, the magnitude distributions may suggest a slightly brighter *1392* component after the peak. If both trails were present and the peak times were correct, then they contributed equal amounts within ~ 30%. The activity curve is not double-peaked, which puts the width of each trail (assumed to be equal) to W = 0.06±0.01 degrees. The

equal contribution implies that the *1405* trail was slightly less shifted backward in time from the assumed A2 effect. At the same time, the *1392* dust trail could be more spread out perpendicular to the Earth's orbit than the factor of 4 derived for the younger Leonid trails.

To our surprise, we do not find a more compact radiant structure for the 2000 outburst Ursids than for the outburst of 1997 (Figure 13). In fact, the overall dispersion in larger. We do not see the meteoroids with the very high right ascension RA > 225 (3 orbits in 1997). Part of the dispersion may be due to a contribution from older dust trails, because in 1997 there were no radiants with RA < 215 (8 orbits in 2000). Our investigation shows that the dust is older than 1000 years. Further work is needed to estimate the age of this debris. The model would be further improved if an explanation could be found for the observed dispersion of radiant positions, reflected in a grouping of low and high inclinations in the meteoroid orbits.

ACKNOWLEDGEMENTS

We thank observers of the California Meteor Society and the Dutch Meteor Society for support of the December 1994, 1997, and 2000 Ursid campaigns reported in this work. We thank all observers in Global-MS-Net that contributed data to this work. PJ acknowledges support from NASA's Planetary Atmospheres and Exobiology programs.

REFERENCES

Asher, D.J., M.E. Bailey, and V.V. Emel'yanenko 1999. Resonant meteoroids from Comet Tempel-Tuttle in 1333: The cause of the unexpected Leonid outburst in 1998. *MNRAS* **304** L53-L56.

Becvár, A. 1946. Circ. IAU No. 1026.

Borovicka, R., R. Stork, and J. Bocek 1999. First results from video spectroscopy of 1998 Leonid meteors. *Meteoritics & Planetary Science* **34**, 987-994.

Brown, P., and R. Arlt 2000. Detailed visual observations and modelling of the 1998 Leonid shower. *MNRAS* **319**, 419-428.

Ceplecha, Z., J. Borovicka, W.G. Elford, D.O. Revelle, R.L. Hawkes, V. Porubcan, and M. Simek 1998. Meteor phenomena and bodies. *Space Sci. Rev.* **84**, 327-471.

Ceplecha, Z. 1951. Umids-Becvar's Meteor stream. *Bull. Astron. Inst. of Czechosl.* **2**, 156-159.

Denning, W. F. 1912. Meteors on Christmas Night Ursids. *The Observatory* **35**, 90-91.

Denning, W. F. 1921. Meteor Notes, Dec. 1920. *The Observatory* **44**, 31-32.

Jenniskens, P. 1987. Ursiden 1986, *Radiant, the Journal of the Dutch Meteor Society* **10**, 101-102

Jenniskens, P. 1994. Meteor stream activity. I. The annual streams. *Astron. Astrophys.* **287**, 990-1013.

Jenniskens, P.1995. Meteor stream activity. II. Meteor outbursts. *Astron. Astrophys.* **295**, 206-235.

Jenniskens, P. 1997. Meteor stream activity IV. Meteor outbursts and the reflex motion of the Sun. *Astron. Astrophys.* **317**, 953-961.

Jenniskens, P. 1998a. First results of Global-MS-Net: Annual Report for 1997. *WGN, the Journal of the IMO* **26**, 79-85.

Jenniskens, P. 1998b. On the dynamics of meteoroid streams. *Earth Planets Space* **50**, 555-567.

Jenniskens, P. 1998c. Ursiden 1997, *Radiant, the Journal of the Dutch Meteor Society* **10**, 21-22.

Jenniskens, P. 2000a. Ursid meteors 2000. IAU Circ. 7544, D.W.E. Green (ed.), December 18, 2000.

Jenniskens, P. 2000b. Ursid meteors 2000. IAU Circ. 7548, D.W.E. Green (ed.), December 23, 2000.

Jenniskens, P. 2001. Discoveries from Observations and Modeling of the 1998/99 Leonids. Contributed Chapter to: *Interplanetary Dust*, E. Grün, B. Å. S. Gustafson eds. (Springer Verlag).

Jenniskens, P., and H. Betlem 2000. Massive remnant of evolved cometary dust trail detected in the orbit of Halley-type comet 55P/Tempel-Tuttle. *Astrophysical Journal* **531**, 1161-1167.

Jenniskens, P., and B.Å.S. Gustafson 2000. The rare 1932 dust trail encounter of 2000 November 17 as observed from aircraft. *WGN, the Journal of the IMO*, **28**, 209-211.

Jenniskens, P., and E. Lyytinen 2000. Possible Ursid outburst on December 22, 2000. *WGN, the Journal of IMO* **28**, 221-226.

Jenniskens, P., and E. Lyytinen 2001. 2000 Ursid outburst confirmed. *WGN, the Journal of the IMO* **29**, 41-45.

Jenniskens, P., H. Betlem, M. de Lignie, and M. Langbroek 1997a. The detection of a dust trail in the orbit of an Earth-threatening Long-period comet. *Astrophys. J.* **479**, 441-447.

Jenniskens, P., H. Betlem, M. de Lignie, C. ter Kuile, M.C.A. van Vliet, J. van 't Leven, M. Koop, E. Morales, and T. Rice 1998. On the unusual activity of the Perseid meteor shower (1989-96) and the dust trail of comet 109P/Swift-Tuttle. *MNRAS* **301**, 941-954.

Jenniskens, P., C. Crawford, S.J. Butow, D. Nugent, M. Koop, D. Holman, J. Houston, K. Jobse, G. Kronk, K. Beatty 2000. Lorentz shaped comet dust trail cross section from new hybrid visual and video meteor counting technique - implictaions for future Leonid storm encounters. *Earth, Moon and Planets* **82-83**, 191-208.

Jenniskens, P., M.A. Wilson, D. Packan, C.O. Laux, C.H. Krüger, I.D. Boyd, O.P. Popova, and M. Fonda 2000. Meteors: a delivery mechanism of organic matter to the Early Earth. *Earth, Moon and Planets* **82-83**, 57-70.

Kondrat'eva, E.D., and E.A. Reznikov 1985. Comet Tempel-Tuttle and the Leonid meteor swarm. *Solar System Research* **31**, 496-492.

Kresák, L. 1993. Cometary dust trails and meteor storms. *Astron. Astrophys.* **279**, 646-660.

Langbroek, M. 1997. Conspicuous Ursid rates in 1996. *International Meteor Conference*, poster presentation (IMO)

Lyytinen, E.J. 1999. Meteor predictions for the years 1999-2007 with the satellite model of comets. *Meta Research Bulletin* **8**, 33-40.

Lyytinen, E.J., and T. van Flandern 2000. Predicting the strength of Leonid outbursts. *Earth, Moon and Planets* **82-83**, 149-166.

Marsden, B.G. 1999. Catalogue of Cometary Orbits, Enslow Publ.

McKinley, D.W.R. 1961. *Meteor Science and Engineering. McGraw-Hill*, New York, 63-68.

McNaught, R.H., and D.J. Asher. 1999, Leonid Dust Trails and Meteor Storms. *WGN Journal of the IMO* **27**, 85-102.

Murray I.S., R.L. Hawkes, and P. Jenniskens 1999. Airborne intensified charge-coupled device observations of the 1998 Leonid shower. *Meteoritics & Plan. Sci* **34**, 949-958.

Murray I.S., M. Beech, M.J. Taylor, P. Jenniskens, and R.L. Hawkes 2000. Comparison of 1998 and 1999 Leonid light curve morphology and meteoroid structure. *Earth, Moon and Planets* **82-83**, 351-367.

Ohtsuka, K. 1994. Expectation for enhancement of the Ursids activity in 1994. *Tokyo Meteor Network Report* no. 14, October 1994, p. 85.

Ohtsuka, K., H. Shioi, E. and Hidaka 1995. Enhanced Activity of the 1994 Ursids from Japan. *WGN, the Journal of IMO* **23**, 69-72.

Williams I.P., and Z.Wu 1994. The current Perseid meteor shower. *MNRAS* **269**, 524-528.

TABLE I

Orbital elements of Ursid meteors (J2000). Mv is the absolute visual magntiude at D=100 km, q = perihelion distance, a = semi-major axis, i = inclination, w = argument of perihelion, Vg is the geocentric velocity after subtraction of the effects of Earth's gravity, RA and DEC are the geocentric radiant positions corrected for the effects of Earth's gravity, while Hb and He are the beginning and end point of the video trajectories.

Code	Node	Mv	q	±	1/a	±	i	±	w	±	Vg	±	Rageo	±	DECgeo	±	Hb	He
1997																		
97600	270.5500	3	0.937	0.002	0.20	0.03	53.8	0.4	206.6	0.6	33.6	0.4	216.4	1.1	75.0	0.2	107.4	94.8
97603	270.5600	5	0.952	0.003	0.20	0.05	51.5	0.9	201.8	1.0	32.3	0.8	228.3	2.0	75.0	0.5	105.7	99.7
97605	270.6000	3	0.951	0.002	0.27	0.06	51.0	1.1	202.8	0.7	31.5	1.0	226.4	1.1	74.5	0.3	104.5	94.0
97610	270.6300	6	0.944	0.007	0.28	0.06	50.7	1.1	205.1	2.3	31.3	0.9	223.1	4.3	75.4	0.7	103.2	99.3
97611	270.6300	4	0.945	0.002	0.26	0.02	51.5	0.5	204.8	0.6	31.9	0.4	222.4	0.9	74.9	0.2	107.7	93.2
97613	270.6400	3	0.942	0.002	0.17	0.03	52.7	0.4	204.9	0.7	33.3	0.4	221.1	1.4	75.7	0.2	105.2	92.8
97618	270.6500	4	0.935	0.005	0.24	0.04	51.5	0.8	207.5	1.4	32.2	0.7	217.7	2.7	76.2	0.4	103.1	95.9
97619	270.7000	4	0.953	0.003	0.24	0.08	51.2	1.5	201.7	1.4	31.8	1.4	227.9	2.2	74.4	0.3	101.2	94.4
97622	270.7100	0	0.944	0.002	0.16	0.03	53.0	0.4	204.2	0.6	33.4	0.4	221.8	1.0	75.3	0.1	108.4	88.3
97625	270.7200	2	0.939	0.002	0.20	0.03	53.4	0.5	206.1	0.6	33.4	0.4	217.9	1.0	75.0	0.2	102.8	89.6
2000																		
20506	270.5926	2	0.949	0.004	0.16	0.04	54.0	0.6	202.5	1.5	33.9	0.4	223.2	2.8	74.1	0.5	107.0	99.4
20513	270.6176	4	0.939	0.002	0.15	0.05	52.1	0.8	205.5	0.6	33.1	0.7	221.0	1.0	76.6	0.3	103.7	94.7
20515	270.6260	4	0.940	0.002	0.30	0.05	51.5	0.9	206.7	0.8	31.6	0.7	219.0	0.9	74.8	0.5	103.0	94.6
20518	270.6391	4	0.941	0.002	0.19	0.06	53.5	1.1	205.3	0.8	33.5	0.9	219.0	0.7	74.8	0.6	102.9	92.4
20521	270.6455	3	0.939	0.002	0.35	0.06	51.5	1.3	207.6	1.0	31.2	1.0	217.6	0.7	74.1	0.4	104.3	92.5
20525	270.6577	2	0.946	0.001	0.30	0.12	51.3	2.5	204.8	1.5	31.5	2.1	222.3	0.4	74.4	0.3	111.3	81.4
20526	270.6610	3	0.943	0.002	0.21	0.06	51.3	1.1	205.0	0.8	32.2	0.9	223.0	1.2	76.0	0.4	103.6	95.6
20527	270.6695	5	0.945	0.002	0.13	0.03	55.2	0.5	203.9	0.6	34.8	0.4	219.4	0.9	74.1	0.5	104.1	96.3
20528	270.6714	5	0.940	0.002	0.34	0.08	50.4	1.8	207.0	1.2	30.8	1.4	219.9	0.6	75.0	0.3	104.9	93.3
20532	270.6775	3	0.941	0.003	0.24	0.14	52.0	2.6	205.9	1.7	32.3	2.2	220.0	1.1	75.3	0.5	104.7	95.3
20536	270.6853	4	0.934	0.002	0.23	0.06	51.4	1.1	207.9	0.8	32.2	0.9	217.1	0.9	76.5	0.5	102.2	93.8
20537	270.6872	5	0.941	0.002	0.24	0.05	51.7	0.9	205.7	0.7	32.2	0.7	220.6	0.8	75.4	0.5	103.7	95.3
20539	270.6882	3	0.934	0.006	0.29	0.10	51.6	1.9	208.4	2.3	31.8	1.5	215.9	3.3	75.3	1.0	108.0	91.5
20540	270.6885	4	0.933	0.002	0.17	0.05	50.5	0.9	207.5	0.7	32.2	0.8	219.4	0.9	78.0	0.4	104.3	95.2
20542	270.6996	2	0.941	0.000	0.22	0.02	52.5	0.5	205.6	0.3	32.7	0.4	219.9	0.0	75.2	0.0	108.2	87.1
20701	270.7212	3	0.946	0.001	0.22	0.03	52.8	0.5	204.2	0.4	32.9	0.5	221.7	0.6	74.5	0.3	107.0	98.0
20703	270.7447	3	0.934	0.001	0.19	0.06	52.4	0.9	207.2	0.6	33.0	0.8	217.1	0.8	76.3	0.2	107.6	100.8
20704	270.7460	2	0.940	0.001	0.23	0.04	51.6	0.6	205.9	0.5	32.2	0.6	220.6	0.8	75.7	0.2	112.7	95.3
20705	270.7478	4	0.928	0.003	0.21	0.03	52.4	0.4	209.2	0.8	33.0	0.4	213.0	1.7	76.4	0.2	108.5	100.4
20706	270.7495	4	0.946	0.001	0.29	0.03	51.6	0.5	204.6	0.5	31.7	0.4	222.1	0.9	74.3	0.2	106.7	98.5
20707	270.7591	6	0.938	0.001	0.20	0.09	53.0	1.5	206.3	0.9	33.2	1.4	217.9	0.7	75.3	0.3	107.9	102.5
20708	270.7599	4	0.944	0.001	0.29	0.03	51.9	0.4	205.3	0.4	31.9	0.4	220.8	0.6	74.4	0.3	107.8	99.5
20709	270.7609	3	0.935	0.001	0.13	0.05	52.5	0.7	206.5	0.4	33.5	0.7	218.5	0.7	76.9	0.3	109.7	98.1
20710	270.7657	5	0.949	0.001	0.23	0.04	52.0	0.6	203.1	0.4	32.4	0.5	224.8	0.7	74.6	0.2	105.7	100.7
20711	270.7662	5	0.944	0.001	0.27	0.03	52.2	0.4	205.1	0.5	32.2	0.4	220.7	0.8	74.4	0.2	106.3	97.9
20712	270.7747	4	0.937	0.002	0.27	0.05	51.4	0.9	207.3	0.7	31.8	0.8	218.1	1.0	75.6	0.2	107.0	99.9
20713	270.7836	5	0.927	0.002	0.15	0.09	54.4	1.4	208.8	0.9	34.5	1.3	211.2	1.0	75.7	0.2	105.1	99.8
20714	270.7837	4	0.943	0.002	0.12	0.03	52.4	0.4	204.4	0.5	33.4	0.4	223.1	1.1	76.3	0.2	107.5	98.9
20715	270.7879	5	0.941	0.001	0.21	0.04	52.2	0.7	205.4	0.5	32.7	0.6	220.5	0.7	75.4	0.3	106.7	99.8
20716	270.7907	4	0.924	0.002	0.14	0.04	54.4	0.6	209.7	0.6	34.5	0.6	209.4	1.1	76.1	0.2	108.1	97.6
20717	270.7918	4	0.934	0.002	0.28	0.03	52.0	0.5	208.1	0.6	32.1	0.4	215.9	0.9	75.3	0.2	105.9	100.3
20718	270.7919	1	0.942	0.001	0.22	0.03	53.0	0.4	205.1	0.5	33.0	0.4	219.9	0.8	74.7	0.2	111.5	92.7
20719	270.8081	4	0.935	0.001	0.17	0.11	53.2	1.8	206.9	1.0	33.6	1.6	216.6	0.8	75.9	0.2	105.5	96.9
20720	270.8089	4	0.929	0.002	0.13	0.05	54.1	0.8	208.3	0.6	34.4	0.7	212.7	1.0	76.2	0.2	105.4	97.8
20721	270.8182	2	0.947	0.001	0.19	0.03	52.9	0.4	203.4	0.5	33.1	0.4	223.0	0.9	74.6	0.2	105.4	99.2
20722	270.8198	4	0.941	0.001	0.13	0.10	54.1	1.6	205.0	0.9	34.3	1.5	219.0	0.9	75.2	0.2	104.9	98.2
20723	270.7280	4	0.940	0.001	0.33	0.03	51.7	0.6	207.0	0.6	31.5	0.5	218.3	0.8	74.2	0.2	105.9	99.0
20725	270.7495	3	0.937	0.001	0.25	0.03	52.0	0.5	206.6	0.5	32.6	0.4	218.8	0.9	76.1	0.2	111.5	95.8
20726	270.7622	3	0.943	0.002	0.17	0.06	53.2	0.9	204.6	0.6	33.5	0.8	220.9	1.0	75.2	0.2	107.9	97.0
20727	270.7643	4	0.941	0.001	0.22	0.03	53.0	0.4	205.5	0.5	33.0	0.4	219.3	0.8	74.8	0.2	106.8	97.6
20728	270.7648	4	0.935	0.002	0.19	0.04	52.7	0.6	207.1	0.5	33.1	0.5	216.9	1.0	75.9	0.2	108.0	97.0
20729	270.7717	1	0.928	0.002	0.15	0.03	53.3	0.4	208.5	0.5	33.9	0.4	213.1	1.1	76.5	0.2	110.5	95.0
20730	270.7746	3	0.938	0.002	0.23	0.05	52.1	0.8	206.4	0.8	32.6	0.7	218.8	1.4	75.6	0.2	106.5	99.3

20731	270.7776	1	0.938	0.001	0.18	0.03	53.2	0.4	206.1	0.5	33.5	0.4	218.0	0.9	75.5	0.2	111.3	91.9
20733	270.7904	4	0.946	0.001	0.19	0.03	52.1	0.5	204.0	0.5	32.7	0.4	223.5	0.9	75.3	0.2	107.1	98.0
20734	270.7928	4	0.944	0.001	0.22	0.06	52.8	1.1	204.7	0.7	32.9	1.0	220.8	0.9	74.6	0.2	105.8	98.1
20735	270.7955	4	0.922	0.003	0.22	0.03	53.5	0.4	210.8	0.8	33.5	0.4	208.7	1.5	75.8	0.2	106.8	100.0
20736	270.8068	2	0.941	0.002	0.21	0.03	52.1	0.4	205.7	0.5	32.7	0.4	220.4	1.0	75.6	0.2	110.6	93.0
20738	270.8092	4	0.948	0.002	0.21	0.03	53.0	0.4	203.4	0.7	33.0	0.4	222.8	1.2	74.2	0.2	106.7	99.5
20739	270.8126	2	0.937	0.002	0.19	0.03	52.4	0.4	206.7	0.6	33.0	0.4	218.1	1.0	75.9	0.2	108.8	93.8
20740	270.8147	3	0.926	0.002	0.21	0.03	53.2	0.5	209.7	0.6	33.4	0.4	211.1	1.1	75.9	0.1	106.4	95.8
20741	270.8196	1	0.939	0.002	0.15	0.03	53.5	0.4	205.7	0.5	33.8	0.4	218.4	1.0	75.5	0.2	116.2	85.6
20742	270.8221	2	0.931	0.002	0.20	0.03	53.1	0.4	208.4	0.6	33.3	0.4	213.9	1.1	75.9	0.2	108.2	93.5

Table II

Ursid orbits (J2000) from the 1945 outburst [Ceplecha 1951 - recalculated] and as observed from California during the 1997 Ursid outburst (P. Jenniskens, M. Koop; calculations M. de Lignie).

Year	1945 3 single station (aphelion outburst)	8P/Tuttle 1994	1997 (Filament) median of 10 orbits (perihelion outburst)	2000 59 orbits (aphelion outburst)	2000 *1405* trail model
Date	Dec. 22.773±0.051	June 17.0	Dec. 22.434±0.057	Dec. 22.32±0.06	Dec. 26±3
RAgeo	217.06±0.07	-.-	222.1±4.2	219.0±4.6	-.-
DECgeo	75.63±0.05	-.-	75.0±0.5	75.3±1.8	-.-
V geo	33.47 (assumed)	-.-	32.25±0.87	33.05±1.1	-.-
a	5.716 (assumed)	5.671775	4.62±0.93	4.673±0.98	5.793±0.002
e	0.8363±0.0015	0.824088	0.795±0.040	0.799±0.053	0.8378±0.0001
q	0.9357±0.0002	0.997732	0.944±0.006	0.940±0.009	0.9398±0.0006
incl	53.10±0.03	54.69254	51.5±1.1	52.5±1.9	52.96±0.02
ω	206.73±0.04	206.7028	204.9±2.0	205.9±2.8	205.68±0.11
Ω	271.35±0.05	270.5487	270.64±0.06	270.76±0.06	270.7579±0.0044

FIGURES

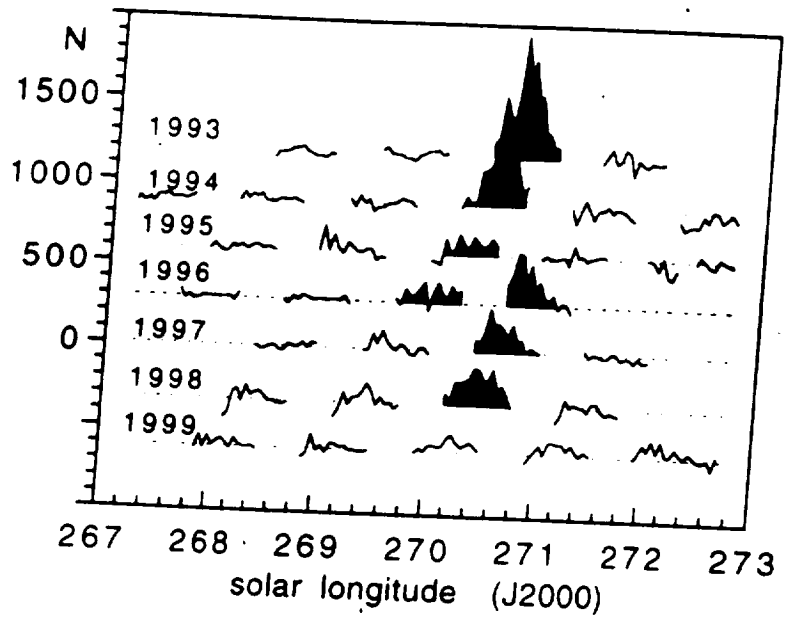

Figure 1a - Ursid Filament as observed around perihelion passage of comet 8P/Tuttle (1994) by forward meteor scatter. Counts (N) are raw reflections after subtraction of the daily background.

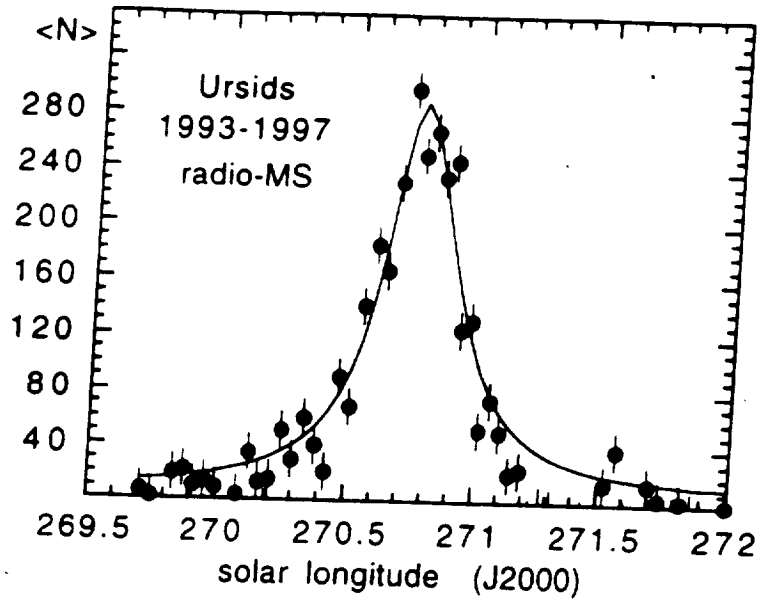

Figure 1b - The mean activity profile of the 1993-1997 outbursts as detected by foreward meteor-scatter, after correction for observability and radiant altitude.

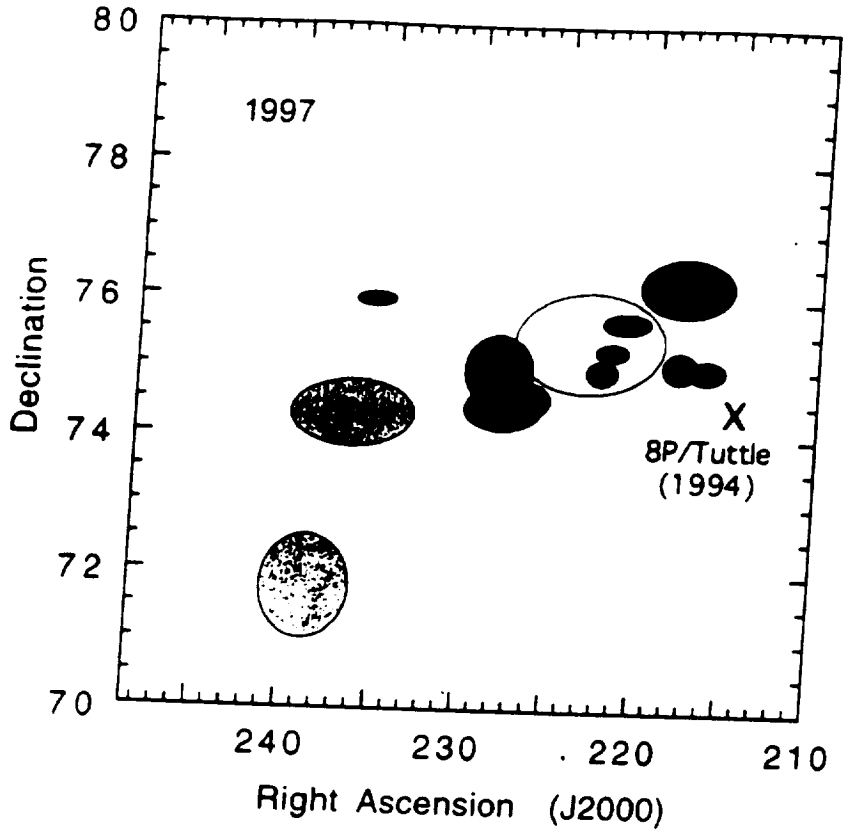

Figure 2 - Radiant positions of 1997 Ursids (Table I). A cross shows the theoretical radiant position derived from the 1994 comet orbit (by allowing a change in q) is indicated.

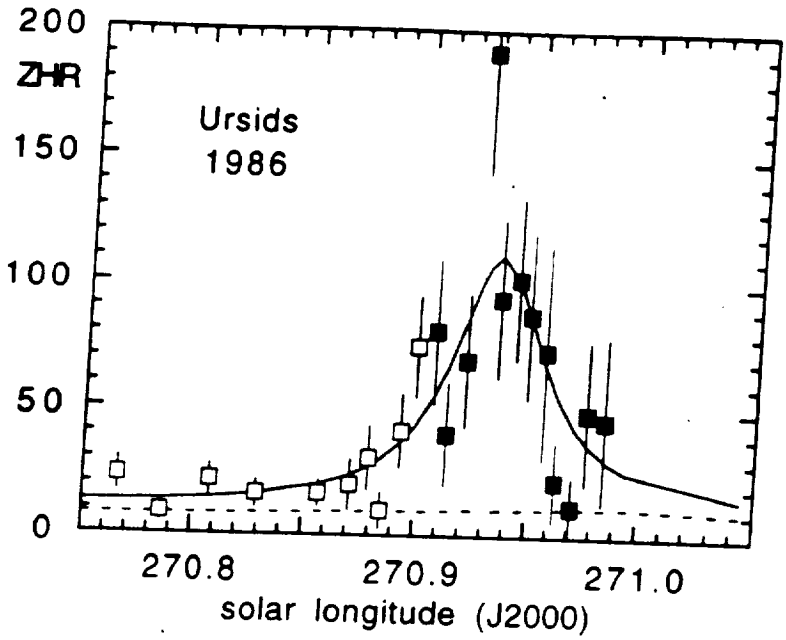

Figure 3 - ZHR curve for the Ursid outburst in 1986 (Jenniskens 1995).

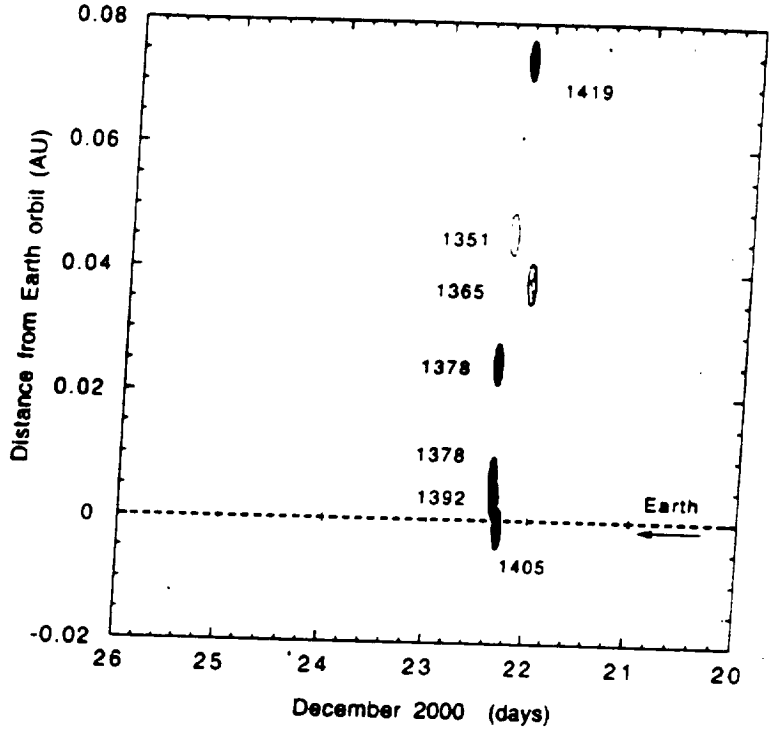

Figure 4 - Position of the various dust trails of 8P/Tuttle relative to the Earth's path (dashed line) in December 2000. The size of the ellipses is twice the expected full-width-at-half maximum.

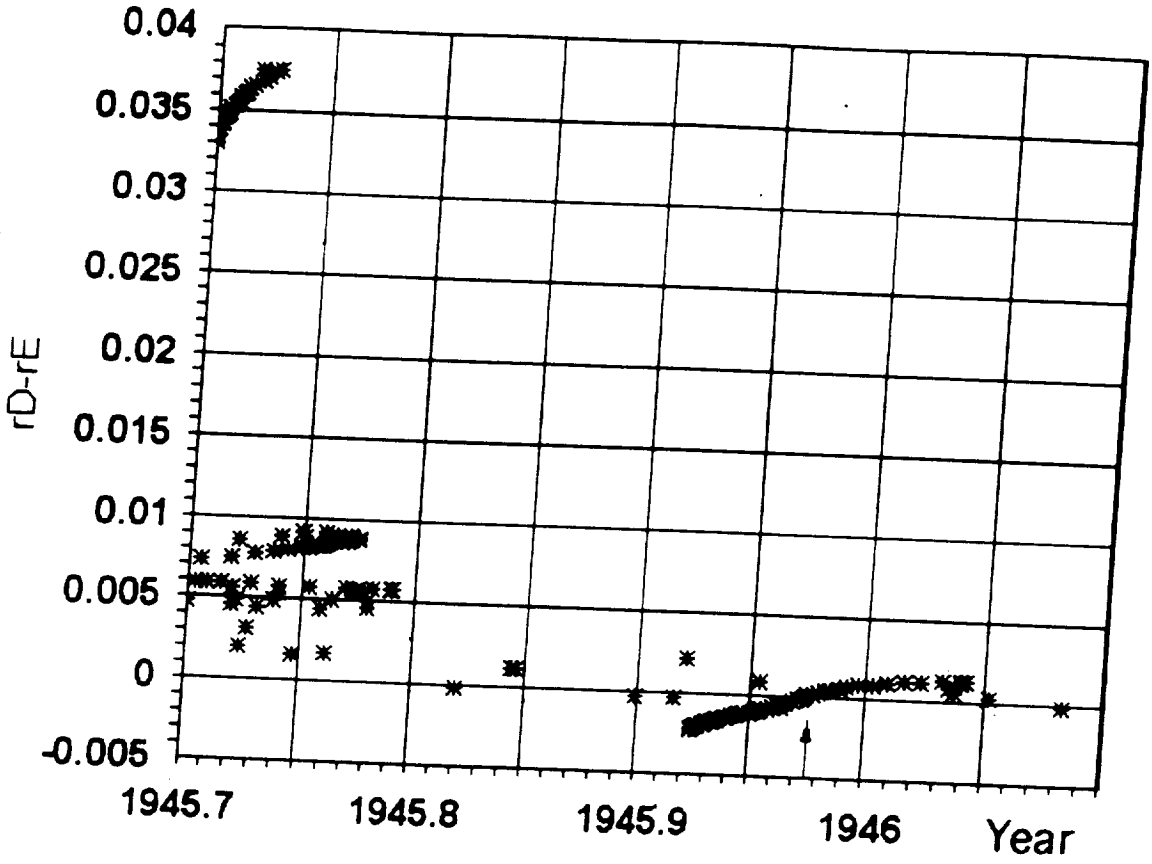

Figure 5 - The *1392* dust trail in a diagram showing the point in time (horizontal axis) and place where the particles cross the ecliptic plane in radial distance from the Sun (vertical axis) around the time of the December 22, 1945 (1945.975) Ursid outburst.

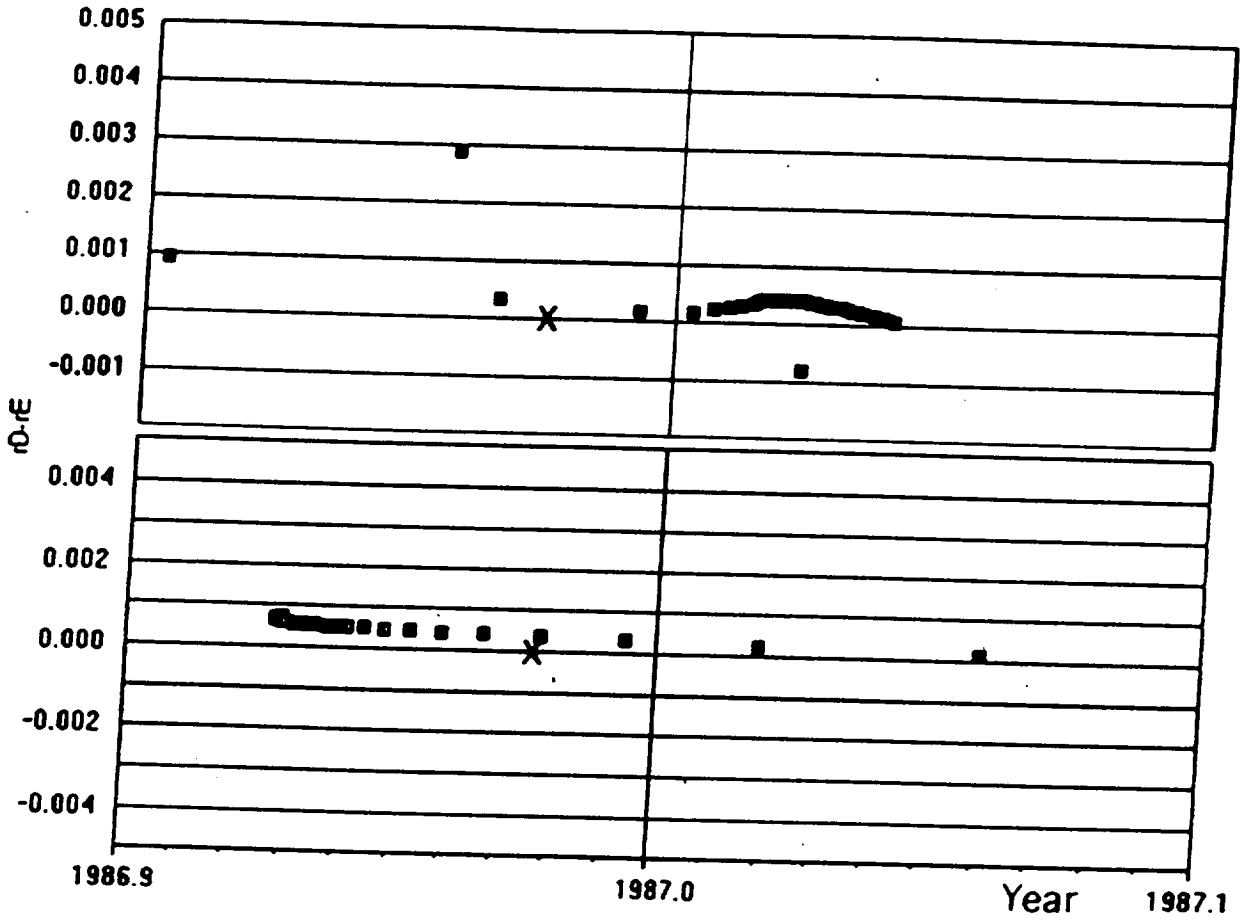

Figure 6 - As figure 5, for two trail fragmens of the dust ejected in *1378* and as encountered during the December 22, 1986 (1986.975) Ursid outburst (cross).

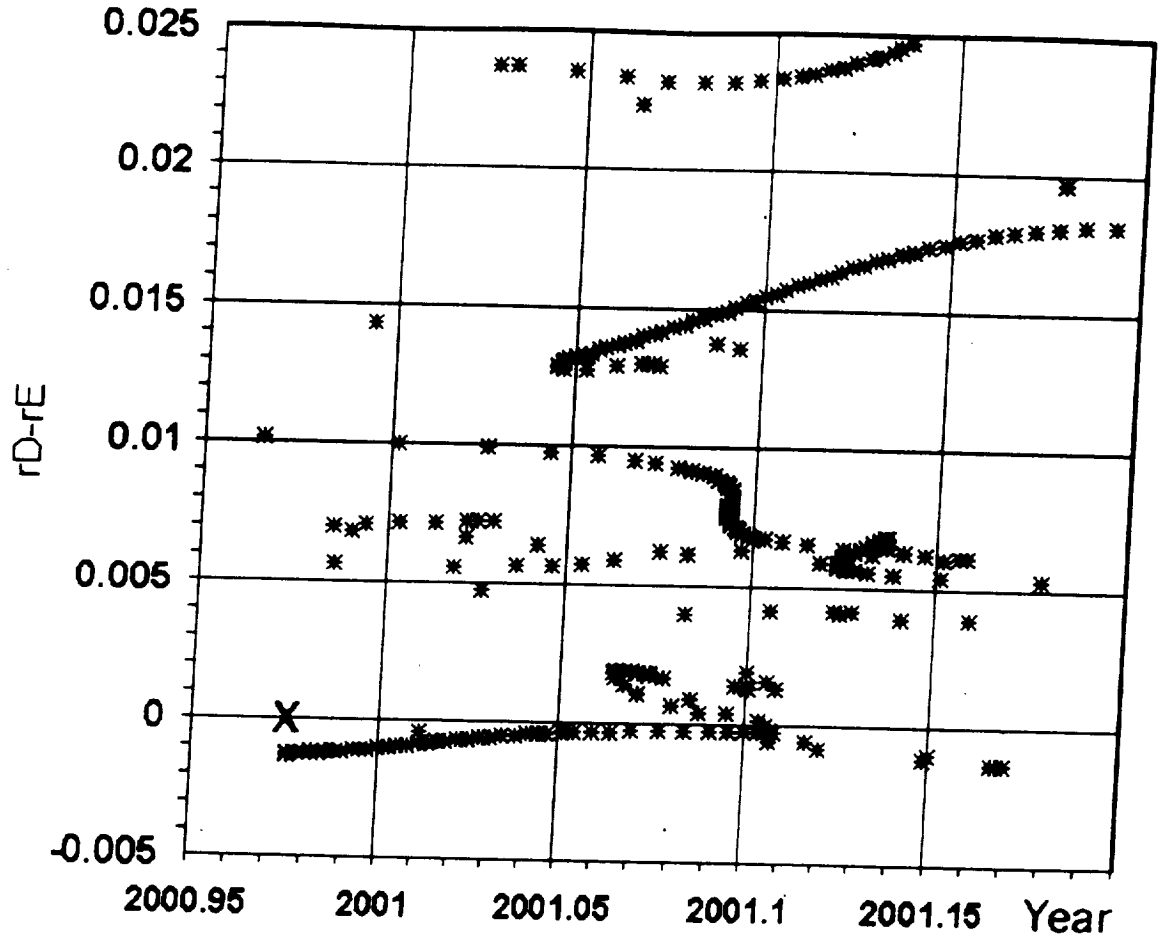

Figure 7 - As figure 5, for the *1405* dust trail as encountered during the December 22, 2000 (2000.975) return.

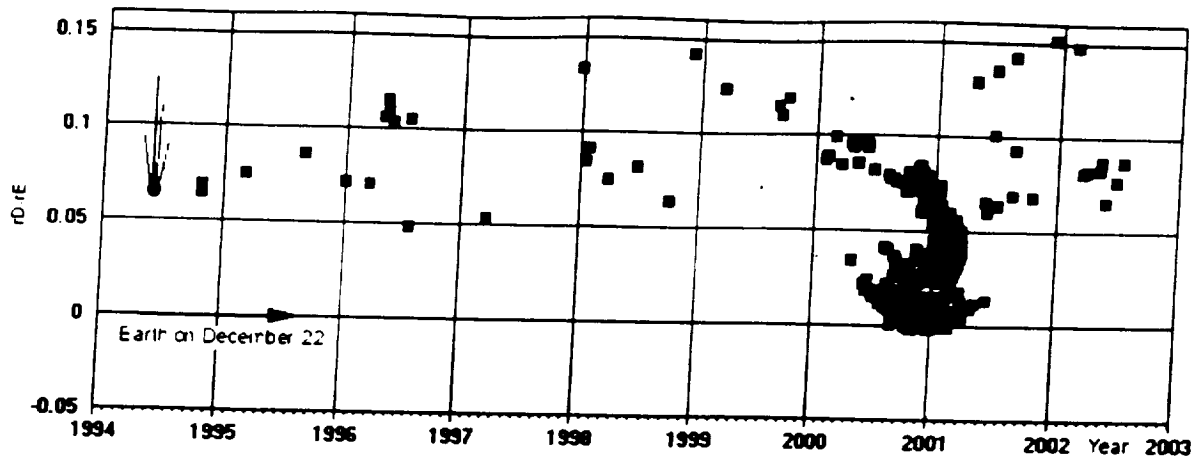

Figure 8 - As figure 5, in a compilation of all test particles for the trails of 1365, *1378*, *1392* and *1405*. Resonances effectively confine the dust to a narrow stream seen only in December 2000, 6 years after the comet's ecliptic plane crossing (comet symbol).

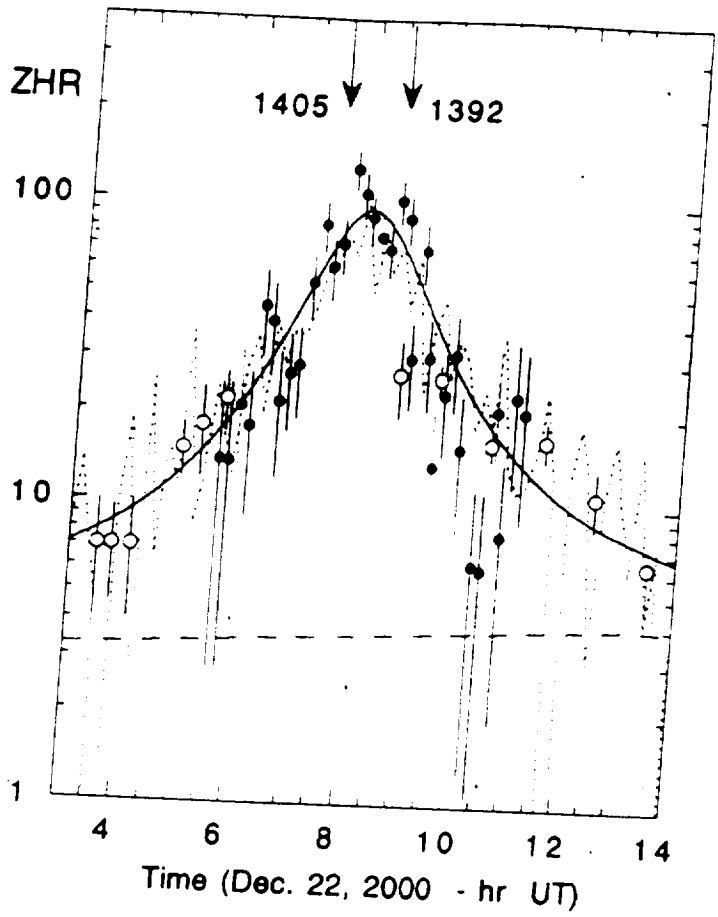

Figure 9 - ZHR curve of Ursids from video (•), visual (o), and radio forward meteor scatter data (---). The dashed line shows the level of annual Ursid activity. The expected peak time for the *1405* and *1392* dust trails is indicated.

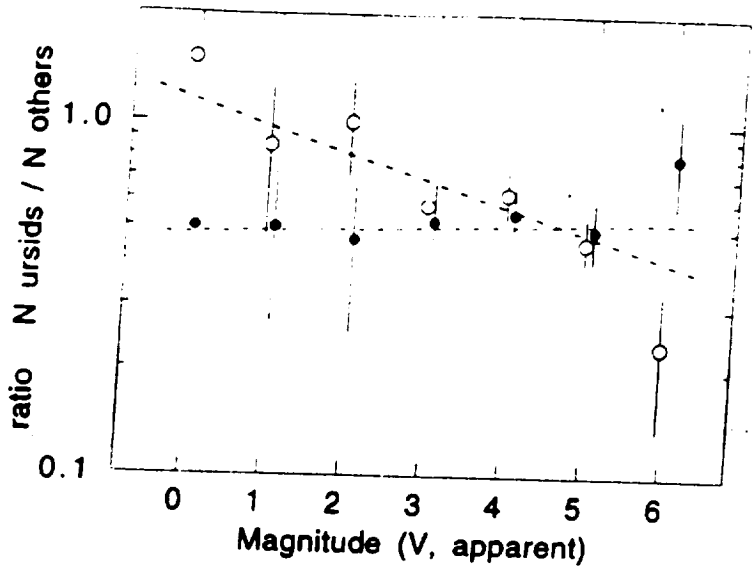

Figure 10 - Apparent magnitude distribution as manifested in the ratio of Ursids and Sporadics for periods prior to (•) and after (o) 8h UT (all cameras).

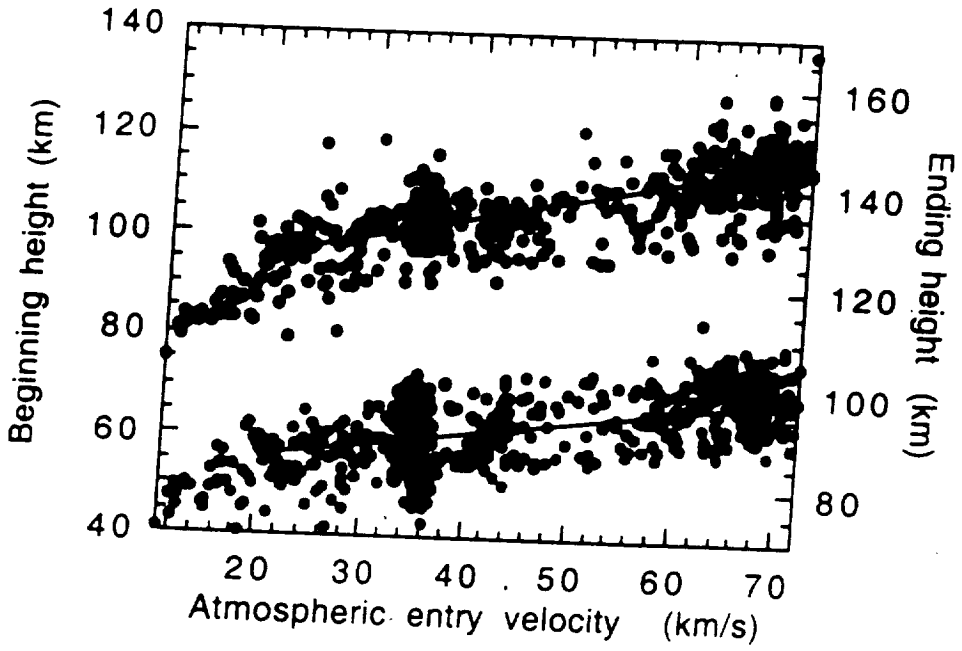

Figure 11 - The beginning and end height of Ursid meteors (black) in relation to other meteors filmed with the same instruments in our database (version 1998).

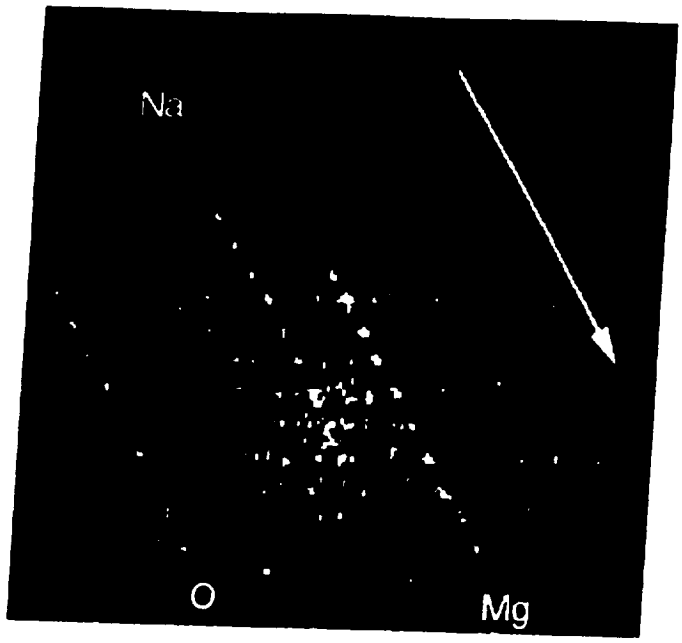

Figure 12 - Compilation of the video spectrum of the 08:24:54 UT Ursid meteor. The wavelength scale runs right to left, while the meteor moved from top left to bottom right. Individual frames show the emission lines of atmospheric oxygen (O), meteoric sodium (Na) and meteoric magnesium (Mg). Diffuse horizontal bands are the atmospheric first-positive bands of the nitrogen molecule.

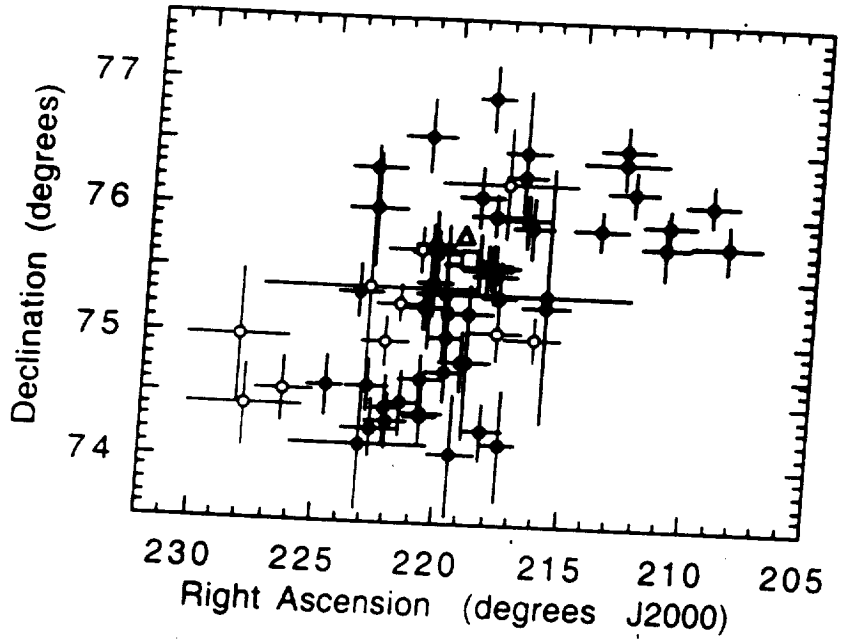

Figure 13 - Radiant positions measured during 2000 Ursid outbust (dark) compared to those measured during 1997 outburst (open circles). An open square and triangle show the expected radiant positions for the *1405* and *1392* dust trails of 8P/Tuttle, respectively.

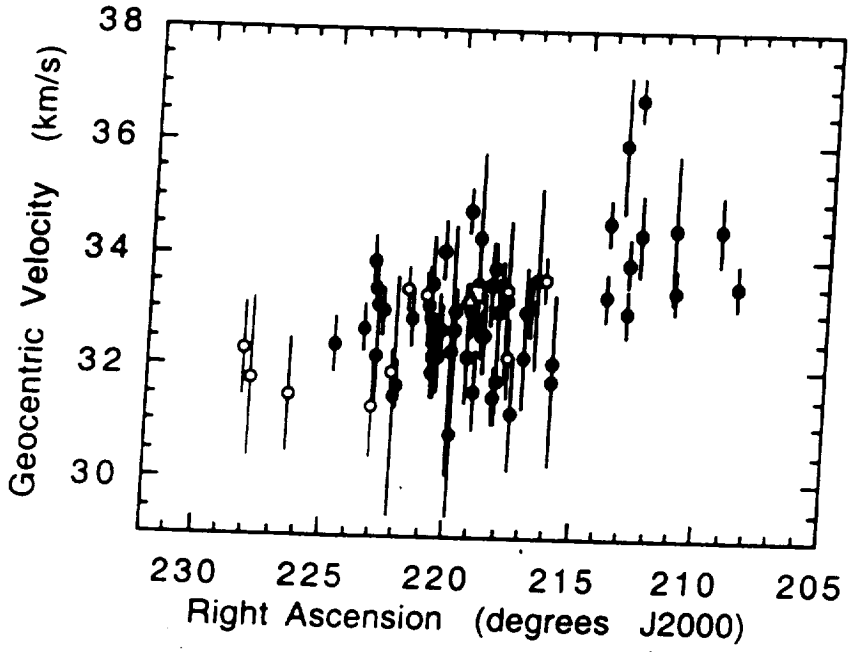

Figure 14 - As Figure 13, for the distribution of meteor speed with radiant Right Ascension.

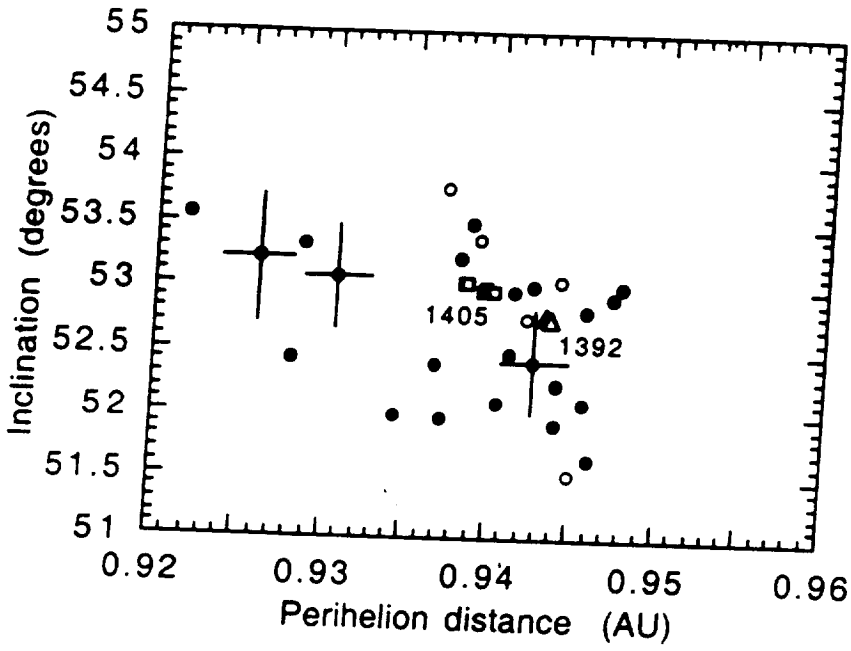

Figure 15 - Symbols as figure 13, for the Distribution of orbital elements in a subset of orbits with precission better than $\sigma i = 0.55$ degrees.

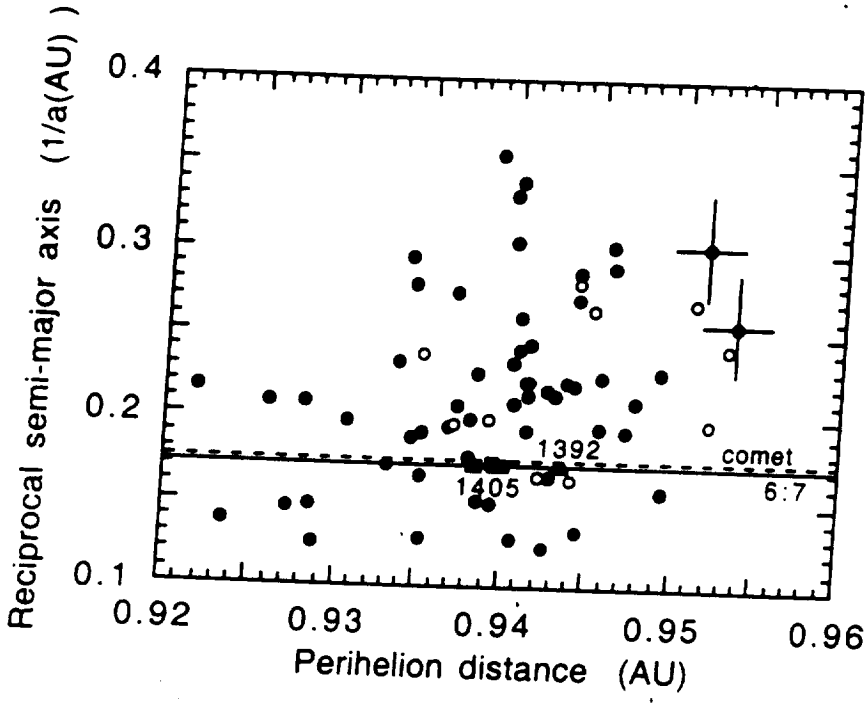

Figure 16 - Symbols as figure 13, for the distribution of semi-major axis versus perihelion distance.